EPJ Photovoltaics **5**, 55205 (2014)
www.epj-pv.org
DOI: 10.1051/epjpv/2014004

Thin metal layer as transparent electrode in n-i-p amorphous silicon solar cells

Martin Theuring[a], Stefan Geissendörfer, Martin Vehse, Karsten von Maydell, and Carsten Agert

NEXT ENERGY – EWE Research Centre for Energy Technology at Carl von Ossietzky University, Carl-von-Ossietzky-Straße 15, 26129 Oldenburg, Germany

Received: 30 July 2013 / Received in final form: 21 January 2014 / Accepted: 10 February 2014
Published online: 7 July 2014

Abstract In this paper, transparent electrodes, based on a thin silver film and a capping layer, are investigated. Low deposition temperature, flexibility and low material costs are the advantages of this type of electrode. Their applicability in structured n-i-p amorphous silicon solar cells is demonstrated in simulation and experiment. The influence of the individual layer thicknesses on the solar cell performance is discussed and approaches for further improvements are given. For the silver film/capping layer electrode, a higher solar cell efficiency could be achieved compared to a reference ZnO:Al front contact.

1 Introduction

Transparent electrodes are used in many electro-optical devices such as displays and solar cells. The main requirements of these electrodes are a low electrical resistance and a high optical transmittance. However, both properties are interdependent, e.g. by the amount of free charge carriers, and improving one usually comes at the expense of the other. For an optimum trade-off between both properties, various different technologies can be applied. The most common approach is the use of degenerate metal oxide semiconductors (TCO: transparent conductive oxide) such as indium tin oxide (ITO). Furthermore, graphene, carbon nanotubes and various types of metal nanostructures are currently under investigation. However, in terms of fabrication those are more complex technologies (review papers on transparent electrodes can be found e.g. from Granqvist [1] and Ellmer [2]).

Solar cells are large area mass products. To be price competitive to other energy technologies, high priced materials and costly fabrication steps have to be avoided. Hence, ITO and sophisticated nanostructures are not suitable for the transparent electrode in these devices. Further cost reductions and new applications can be created with roll-to-roll processing and flexible devices. Yet, this leads to additional requirements for the individual layers in the cell, such as bendability. Temperature-sensitive substrates or absorber layers also limit the possible processing techniques.

However, a transparent electrode is required in thin film solar cells for charge carrier collection. In silicon thin film solar cells highly doped zinc oxides (e.g. AZO: aluminum doped zinc oxide) or tin oxides are often applied for this purpose [3]. To achieve a sufficient conductivity for solar cell applications, thick layers (up to several μm) are needed, which are less flexible. Furthermore, for sputtered AZO an optimized performance will be obtained if the material is deposited on a heated substrate [4]. But a high temperature process can degenerate the underlying layers by decomposition or cracking due to differences in their temperature coefficients.

Amongst others (see [5]), Sahu et al. [6] have shown that the incorporation of a few nanometers of silver in thin TCO layers strongly reduces the sheet resistance, while still providing high optical transmittance in the visible part of the spectrum. Higher mechanical stability and a simple low temperature fabrication process are the advantages of this design [7].

The objective of this paper is to demonstrate the integration of thin metal layers as a transparent electrode in n-i-p amorphous silicon (a-Si) solar cells. In this work, we focus on thin metal layers adjacent to the *p*-layer of the cell. As an anti-reflection (AR) and protection layer, sputtered AZO is compared to an AZO/SiO_x multilayer. We analyze the influence of the individual layers' thicknesses and deduce design rules for an optimized performance.

2 Experimental details

As substrates for the solar cells, we use glass slides with a layer of chemically wet etched, structured AZO. The latter was coated with a 30 nm layer of aluminum followed

[a] e-mail: martin.theuring@next-energy.de

by 50 nm of silver for opaqueness. Both metal layers were deposited by electron beam evaporation. Subsequently, a 70 nm layer of AZO was sputtered on the back contact. Hydrogen-passivated amorphous silicon layers were fabricated in the n-i-p configuration (deposition order: n-doped/intrinsic/p-doped) by plasma-enhanced chemical vapor deposition (PECVD). The cell structure is depicted on the right sides of Figures 1, 3 and 5. SiH_4, H_2 and PH_3 were used as process gases for the n-doped a-Si layer, SiH_4 and H_2 for the intrinsic a-Si layer (i-layer) and SiH_4, CH_4, H_2 and B_2H_6 for the p-doped a-SiC layer, respectively. SiO_x AR-layers were fabricated in a PECVD process at 180 °C substrate temperature. SiH_4, H_2 and CO_2 were used with a dilution rate of CO_2 to SiH_4 of approximately 18.3 to 1, which led to highly transparent, SiO_2-like layers (refractive index n of SiO_x in the range of 1.5–1.6).

The silver layer in the front contact and all AZO layers were deposited by DC magnetron sputtering. We estimate that the deposition rate for the silver layer is approximately 1 nm/s. This value was obtained by measuring a silver layer on a flat substrate by spectroscopic ellipsometry and subsequent modeling. However, the actual layer thickness might be different on structured substrates, such as the solar cells in our experiments. In the following, we therefore only give the deposition times for the silver layers as a rough indication for the layer thicknesses. For the AZO layers, we used a ZnO sputter target with a 2wt% concentration of Al_2O_3. Before the deposition of AZO and silver no substrate heating was used, which is crucial for the thin silver layers. Island formation was observed with heating temperatures exceeding 80 °C, depending on the layer thickness. However, the 700 nm AZO reference layer was deposited on a substrate at 300 °C. All solar cells were annealed at 160 °C for 30 min after fabrication.

We defined the active cell area with the size of the front contact. A marker pen was used to draw square openings with a size of ≈0.65 cm^2 before front contact deposition. The liftoff process was carried out by sonication in an acetone bath. Short circuit current densities (J_{SC}) were obtained from external quantum efficiency (EQE) measurements by convolution with the AM1.5G spectrum. Current density-voltage (JV) curves were measured with a solar simulator under standard test conditions and scaled to the J_{SC} values calculated from the EQE data. Sheet resistances were obtained by four point measurement method.

The simulation results were calculated with the software Scout/Code (by W. Theiss Hard- and Software), which solves the electromagnetic wave equation for the one dimensional case. The layer stack of the solar cell used in the simulation was matched to the experimental data. Simulated EQEs were obtained from the computed absorption in the intrinsic layer. Optical material parameters were partly (Ag, SiO_2) taken from reference [8], partly obtained by spectroscopic ellipsometry and subsequent modeling (all other materials).

3 Results and discussion

3.1 Optimization of the silver layer thickness

As already outlined at the beginning of this paper, the incorporation of a thin metal layer in TCO strongly influences the sheet resistance of the structure and of course, the thicker metal layers lead to lower resistances. However, an increase of the metal layer thickness decreases the transmittance of the device due to higher reflectivity and absorption from the metal [6]. On the other hand, for thinner metal layers the sheet resistance increases nonlinearly with the thickness: scattering at grain boundaries and surface boundaries play a more dominant role [9]. Depending on what kind of metal is used, its thickness and the substrate type, island formation of the metal is observed, which leads to interrupted current paths (see inset of the graph in Fig. 1) [1]. Furthermore, discontinuities in the metal layer allow the excitation of localized surface plasmon polaritons [10]. This reduces the optical transmittance due to an increased absorption in the metal and its proximities.

On the left side of Figure 1, the JV-characteristics of four n-i-p a-Si solar cells are shown (cell composition sketched on the right side of the same figure). In the Figure legend, the corresponding sheet resistances of the front contacts are specified. The cells differ in the deposition time of the silver layer in the transparent front electrode. For 4 s of deposition (red curve) a sheet resistance of $R_{Sq} \approx 1800\ \Omega$ was measured, which is in the range of the sheet resistance of the AZO capping layer. This can be explained with the discontinuity of the silver caused by island formation (SEM image of silver islands is shown in the inset of the graph). This behavior is also confirmed by the cells' JV-characteristics: the red JV-curve is dominated by the high ohmic resistance of the front contact. By increasing the deposition time, the islands connect, resulting in a much lower sheet resistance (e.g. orange curve). When the silver layer thickness is increased beyond an optimal value (optimized sample roughly represented by the green curve), more and more light is reflected by the cell and the maximum value of extractable charge carriers decreases (blue curve). Further research should be directed towards applicable adhesion layers for the metal, which could prevent island formation for thinner silver films [11].

3.2 Influence of anti-reflection capping layer

The application of an AR layer on a thin metal film is essential for a high transmittance of the transparent electrode [7]. The dotted blue line in Figure 2 represents the simulated EQEs of a solar cell stack with only a thin Ag layer as transparent front contact. In comparison the solid green line shows the data from the same device but with an additional AZO layer of optimized thickness for the antireflective coating. Both, the EQE curves as well as the calculated J_{SC} values given in the table inset demonstrate the necessity of the capping layer. The data from

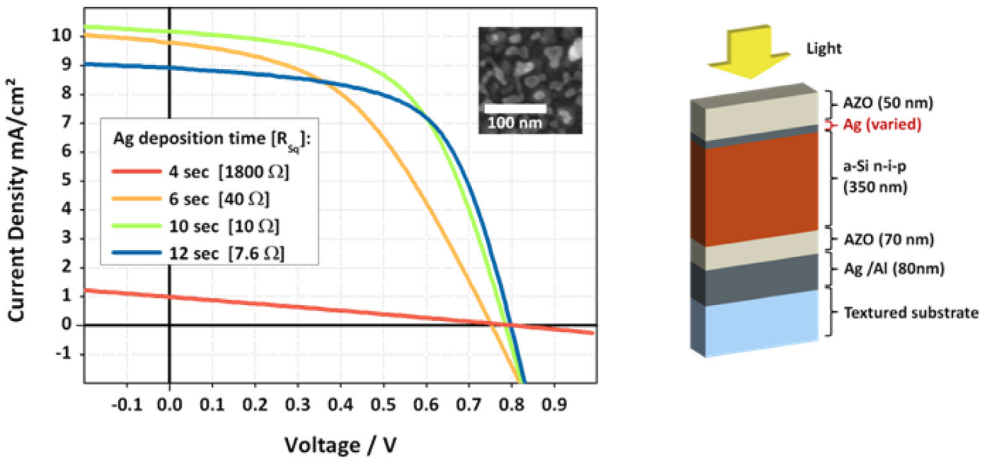

Fig. 1. Variation of the silver layer thickness of the front contact. Left: JV-characteristics of the solar cells (approximate front contact sheet resistance in parentheses; inset: example for island formation in thin Ag layers [scanning electron microscope image]). Right: Design of the solar cell stack (individual layer thicknesses in parentheses).

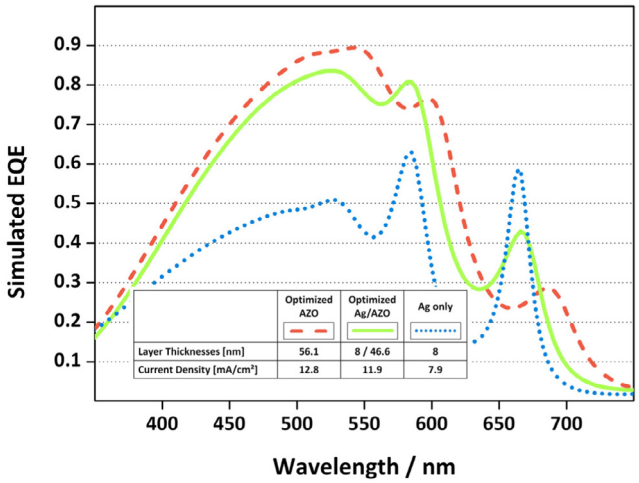

Fig. 2. Simulated external quantum efficiencies for solar cells with different front contacts. Table inset contains layer thicknesses of the different front contacts and the calculated current density of the devices.

a solar cell stack with only a thin AZO layer optimized for antireflective quality is also shown in the same graph. Without the silver layer, the obtained J_{SC} is almost identical to the Ag/AZO sample. For this cell, the high sheet resistance of the front electrode would not allow a good current extraction.

The thickness of the AR-coating material and its optical density play a key role for the solar cell performance. The computed results clearly show the influence of the front contact on the optical properties of the solar cell. However, the results obtained from the 1D-simulation cannot directly be adapted to the experiment. Here, light trapping mechanisms are employed, which augment the spectral response of the solar cell for longer wavelengths. Also the optical cavity of the thin film stack, which causes the optical interference peaks visible in the simulation results, is weakened due to the light scattering at the textured back contact. The curves in Figure 3 show the EQE and 1-total cell reflectivity (1-R) values for a variation of the AZO capping layer thickness in 10 nm steps. Towards the red spectral band the absorption coefficient of a-Si decreases. For wavelengths above 750 nm, almost no charge carriers are generated in the absorber layer (i-layer). The light is transmitted to the back electrode, where it is mainly absorbed at the structured silver back contact [12].

With increasing AZO layer thickness, the reflectivity peak around 350 nm grows larger. This behavior is directly translated to the EQE curves of the cells: the EQE for shorter wavelengths is reduced. But even for good AR-properties (40 nm AZO sample), a comparably low efficiency is found. In this spectral range, the light is partly absorbed, before reaching the absorber layer. In Figure 4, the simulated absorption distribution in a solar cell is depicted for the 1D case. A large part of the parasitic absorption occurs in the doped layers, where most excited electrons recombine due to high defect densities. Further optimization of these layers helps to overcome such problems, which however, is not the objective of this study.

A full understanding of parasitic absorption in the investigated solar cells is still not given. The simulation results suggest that considerable parasitic absorption can also be attributed to the thin metal film. For thin film optics, the mode distribution in the individual layers plays a key role. Additionally, the influence of the surface roughness on the thin metal film and the light interaction with non-flat metal layers require further investigations. But also the AZO layer is responsible for parasitic absorption. Especially for lower deposition temperatures, which are required for this application, the AZO's transmittance decreases for shorter wavelengths [4].

Therefore, we applied an advanced capping layer, consisting of an AZO/SiO_x double structure. The AZO is required to prevent island formation of the silver layer, as

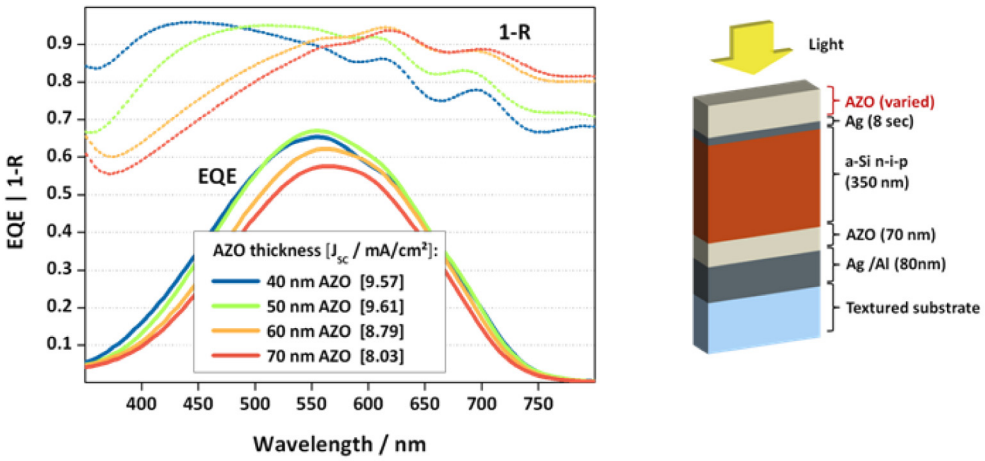

Fig. 3. Thickness variation of the aluminum zinc oxide (AZO) layer in the front contact. Left: External quantum efficiency and 1-total cell reflectivity (short circuit current densities of the corresponding cells in parentheses). Right: Design of the solar cell stack (individual layer thicknesses in parentheses).

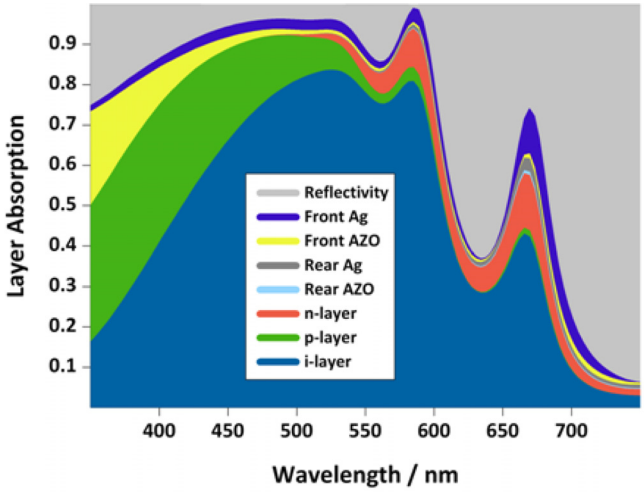

Fig. 4. Simulated absorption distribution in the individual layers of a n-i-p solar cell with Ag/AZO front contact.

the SiO_x was deposited at elevated temperatures. In order to investigate the influence of the capping layer, we performed a thickness variation of the SiO_x layer. The results of this experiment are depicted on the left side of Figure 5. A similar behavior compared to the AZO variation is found. An increase of the SiO_x layer thickness results in a red shift of the AR properties. The overall reflectivity of the cell is found to be higher with the SiO_x capping layer compared to the Ag/AZO contact (the best performing samples with Ag/AZO and Ag/AZO/SiO_x front contact, respectively, are shown in Fig. 6). However, a gain in efficiency for wavelengths up to approximately 475 nm can be found in direct comparison. For further optimizing the performance, a low-absorptive dielectric with higher n (such as Al_2O_3 or TiO_2) should be considered as capping layer material. Also the use of a different deposition method with lower temperatures could be beneficial. This would allow omitting the remaining 15 nm AZO cover layer and further reduce the parasitic absorption.

Figure 6 also displays the measurement results from a cell with a 700 nm AZO front contact. From Table 1 one can see, that for our experiment, both, the Ag/AZO and the Ag/AZO/SiO_x front contact show a higher efficiency compared to the 700 nm AZO contact. The explanation for this behavior can be found in both, the electrical and optical performance of the front electrode. The sheet resistance of the AZO layer is twice as for the silver-based electrodes. Accordingly, JV-curve and thus the fill factor are influenced negatively. For a lower sheet resistance, a thicker AZO is required which on the other hand would further increase the parasitic absorption in this layer. However, the parasitic loss is already higher for the AZO-only sample. Especially for shorter wavelengths, the EQE is lower while the anti-reflective properties of the contacts are in a comparable range. We, therefore, achieve a higher efficiency with the silver film based transparent electrodes.

4 Conclusion

In this paper it was demonstrated that transparent electrodes based on thin silver films are applicable in structured a-Si solar cells in n-i-p configuration. We narrowed down the possible thicknesses of the silver layer for good optical and electrical performance. The capping layer is crucial for the optical properties of the transparent electrode. Its antireflective properties can be tuned with a thickness or material variation. In this way a higher efficiency can be obtained than with a solar cell with a 700 nm AZO front contact.

The authors would like to thank Volker Steenhoff and Samuel Gage for discussion and Regina Nowak and Tim Möller for discussion and ellipsometry measurements. We would like to

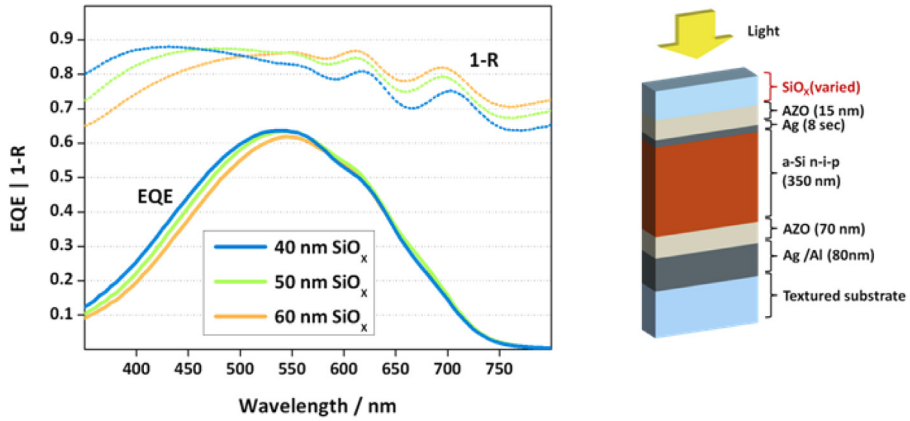

Fig. 5. Variation of the SiO_x layer thickness. Left: External quantum efficiency and 1-total cell reflectivity. Right: Design of the solar cell stack (individual layer thicknesses in parentheses).

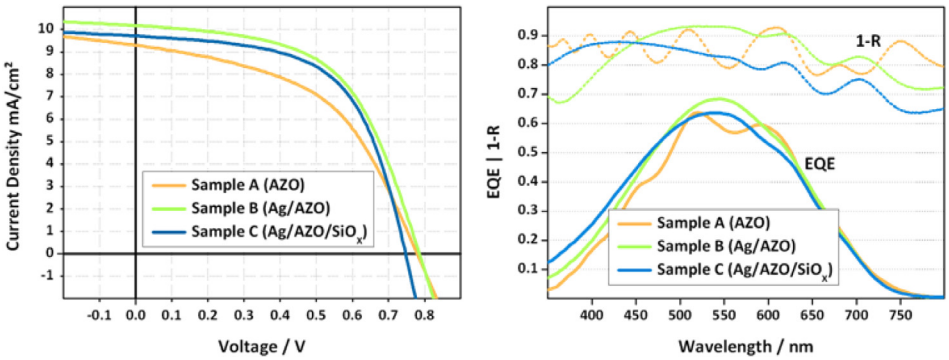

Fig. 6. Comparison of different front contacts (figures of merit see table below). Left: JV-characteristics of the solar cells. Right: External quantum efficiency and 1-total cell reflectivity.

Table 1. Measured cell performance of a-Si solar cells with different front contact. Open circuit voltage (V_{OC}), short circuit current density (J_{SC}), fill factor (FF), sheet resistance of the front contact (R_{Sq}) and cell efficiency (η).

Front Contact (approximate layer thicknesses)	V_{OC} [mV]	J_{SC} [mA/cm^2]	FF [%]	R_{Sq} [Ω]	η [%]
Sample A (700 nm AZO)	779	9.3	49.5	19	3.6
Sample B (8 s Ag/50 nm AZO)	785	10.2	55.7	10	4.5
Sample C (8 s Ag/15 nm AZO/15 nm SiO_x)	747	9.7	58.9	8.3	4.3

thank the BMBF for supporting this work in the framework of the project SiSoFlex (FKZ 03SF0418B).

References

1. C.G. Granqvist, Sol. Energy Mater. Sol. C **91**, 1529 (2007)
2. K. Ellmer, Nat. Photon. **6**, 809 (2012)
3. J. Müller, B. Rech, J. Springer, M. Vanecek, Sol. Energy **77**, 917 (2004)
4. O. Kluth, G. Scho, B. Rech, R. Menner, M. Oertel, K. Orgassa, H. Werner, Thin Solid Films **502**, 311 (2006)
5. C. Guillén, J. Herrero, Thin Solid Films **520**, 1 (2011)
6. D. Sahu, S. Lin, J. Huang, Appl. Surf. Sci. **252**, 7509 (2006)
7. D.S. Ghosh, T.L. Chen, N. Formica, J. Hwang, I. Bruder, V. Pruneri, Sol. Energy Mater. Sol. C **107**, 338 (2012)
8. E.D. Palik, *Handbook of Optical Constants of Solids* (Academic Press, Burlington, 1997)
9. J.R. Sambles, Thin Solid Films **106**, 321 (1983)
10. M. Theuring, M. Vehse, I. Noureddine, K. von Maydell, C. Agert, in *MRS Online Proc. Library* (Cambridge University Press, 2012), Vol. 1426
11. V.J. Logeeswaran, N.P. Kobayashi, M.S. Islam, W. Wu, P. Chaturvedi, N.X. Fang, S.Y. Wang, R.S. Williams, Nano Lett. **9**, 178 (2009)
12. F.-J. Haug, T. Söderström, O. Cubero, V. Terrazzoni-Daudrix, C. Ballif, J. Appl. Phys. **104**, 064509 (2008)

Cite this article as: Martin Theuring, Stefan Geissendörfer, Martin Vehse, Karsten von Maydell, Carsten Agert, Thin metal layer as transparent electrode in n-i-p amorphous silicon solar cells, EPJ Photovoltaics **5**, 55205 (2014).